Journal of Nuclear Science and Technology

ISSN: 0022-3131 (Print) 1881-1248 (Online) Journal homepage: http://www.tandfonline.com/loi/tnst20

Measurement of Response Functions of a Liquid Organic Scintillator for Neutrons up to 800 Me V

Daiki SATOH , Tatsuhiko SATO , Akira ENDO , Yasuhiro YAMAGUCHI , Masashi TAKADA & Kenji ISHIBASHI

To cite this article: Daiki SATOH , Tatsuhiko SATO , Akira ENDO , Yasuhiro YAMAGUCHI , Masashi TAKADA & Kenji ISHIBASHI (2006) Measurement of Response Functions of a Liquid Organic Scintillator for Neutrons up to 800 Me V, Journal of Nuclear Science and Technology, 43:7, 714-719, DOI: 10.1080/18811248.2006.9711153

To link to this article: https://doi.org/10.1080/18811248.2006.9711153

Published online: 05 Jan 2012.

Journal of NUCLEAR SCIENCE and TECHNOLOGY, Vol. 43, No. 7, p. 714–719 (2006)

ORIGINAL PAPER

Measurement of Response Functions of a Liquid Organic Scintillator for Neutrons up to 800 MeV

Daiki SATOH[1,*], Tatsuhiko SATO[1], Akira ENDO[1], Yasuhiro YAMAGUCHI[1], Masashi TAKADA[2] and Kenji ISHIBASHI[3]

[1]*Japan Atomic Energy Agency, Tokai-mura, Naka-gun, Ibaraki 319-1195, Japan*
[2]*National Institute of Radiological Sciences, Anagawa, Inage-ku, Chiba 263-8555, Japan*
[3]*Kyushu University, Hakozaki, Higashi-ku, Fukuoka 812-8581, Japan*

(Received January 16, 2006 and accepted in revised form March 24, 2006)

Response functions of a BC501A liquid organic scintillator for neutrons up to 800 MeV have been measured at the heavy-ion accelerator of the National Institute of Radiological Sciences, Japan. A thick graphite target was bombarded with 400-MeV/u C ions and 800-MeV/u Si ions to produce high-energy neutrons whose kinetic energy was determined by the time-of-flight method. The measured response functions were compared with the results obtained using SCINFUL-QMD code, and the accuracy of the code was experimentally verified up to 800 MeV. This work will contribute to extending the energies measurable with our new radiation dose-monitoring system (DARWIN), which is based on the BC501A scintillator.

KEYWORDS: response function, liquid organic scintillator, BC501A, SCINFUL-QMD, high-energy neutron, DARWIN, radiation monitor

I. Introduction

High-intensity particle accelerators have been constructed or planned for frontier research in areas including particle physics, nuclear engineering, and medical applications. The Japan Atomic Energy Agency (formerly the Japan Atomic Energy Research Institute) and the High Energy Accelerator Research Organization are collaborating to construct the high-intensity proton accelerator complex J-PARC.[1)] At these facilities, neutrons with a wide energy distribution are produced through nuclear spallation by the interactions of high-energy particles with the accelerator components. The radiation dose outside the shielding is dominated by neutrons, and their energies reach several hundred million electron volts.[2)] Therefore, dose monitoring of high-energy neutrons is one of the key issues in radiation protection of workers and the general public.

We have developed a new dose-monitoring system applicable to various types of radiation over a wide energy range (DARWIN)[3)] for monitoring doses from neutrons, photons, and muons in the workspaces and surrounding environments of accelerator facilities. A BC501A liquid organic scintillator was employed as a radiation detector for neutrons above 1.2 MeV as well as for photons and muons in DARWIN, because this scintillator has a high detection efficiency and a good capability of distinguishing neutrons and photons. The neutron dose is assessed from the light output by applying the G-function[4)] that is derived from a set of the response functions of the BC501A scintillator and the dose conversion coefficients. The performance of DARWIN has been verified in the energy region from thermal to 80 MeV[3,5–7)] in various neutron fields. The upper energy limit is determined by the available response function for the scintillator using SCINFUL code,[8)] which evaluates the response function for neutrons from 0.1 to 80 MeV based on a multibody-breakup model.

We previously developed Monte-Carlo-based code, SCINFUL-QMD,[9,10)] that incorporates a quantum molecular dynamics (QMD) model[11)] into SCINFUL to allow it to evaluate the response functions for higher energy neutrons. This code is capable of calculating the response for various sizes of organic scintillator for incident neutron energies up to 3 GeV. Experimental validation of the code is essential when using the response functions calculated by SCINFUL-QMD to extend the neutron energies that are measurable using DARWIN. A few experimental data sets are available for energies above 80 MeV. For example, Nakao *et al.*[12)] measured the response functions using quasi-monoenergetic neutron sources, and Sasaki *et al.*[13)] measured them with spallation neutron sources. While these experimental data are very useful for assessing the capabilities of the code, the data set of Nakao *et al.* is limited to neutron energies up to 206 MeV, and the statistics of the data reported by Sasaki *et al.* is quite degraded for higher energy neutrons, even though they measured up to 800 MeV. For these reasons, the existing experimental data are insufficient for assessing the accuracy of SCINFUL-QMD for energies over several hundred million electron volts.

We therefore measured the response functions of the BC501A scintillator for neutrons up to 800 MeV at the Heavy-Ion Medical Accelerator in Chiba (HIMAC) of the National Institute of Radiological Sciences (NIRS), Japan. The experimental data are compared with the predictions of the SCINFUL-QMD and another Monte-Carlo-based code, CECIL,[14)] which has been widely used to determine

*Corresponding author, E-mail: satoh.daiki@jaea.go.jp

response function above 100 MeV. By use of SCINFUL-QMD, we plan to extending the neutron energy measurable with DARWIN from 80 MeV to 1 GeV.

II. Experimental Setup

The experiment was performed using the PH2 beam line at the HIMAC of the NIRS, with the experimental setup shown in **Fig. 1**. HIMAC is a heavy ion accelerator complex (injector linac and two synchrotron rings) that can supply 100 to 800 MeV/u beam of $q/A=1/2$. 400-MeV/u C ions and 800-MeV/u Si ions were employed as incident heavy ions to generate neutrons at a thick graphite target by spallation reactions. The thicknesses of the targets for the C and Si ions were 20 and 23 cm, respectively, which ensured that the primary ions stopped inside them. The target material was chosen as a compromise between the production rates of neutrons and other fragments. An NE102A plastic scintillator (BM) was placed in front of the target to monitor the heavy-ion beams. The BM was 3 cm in diameter, which was smaller than the front surface of the target to ensure that all tagged particles subsequently entered into the target. The thickness of BM was 0.5 mm so as to reduce the energy loss of incident beam inside it.

A cylindrical BC501A liquid organic scintillator with a diameter of 12.4 cm and a thickness of 12.7 cm was positioned 5.0 m downstream of the target and 15° from the beam axis. Scintillations of the BC501A scintillator are caused by incident neutrons as well as gamma rays and charged particles, which hereafter are referred to neutron, gamma-ray, and charged-particle events, respectively. Since the synchrotron is operated in a pulse mode (0.3 Hz repetition cycle, where flat-top period is 1,230 ms) and the beam intensity can be reduced below 10^5 particles per second, neutrons emitted from the target can be individually counted and their kinetic energies are determined from the time-of-flight (TOF) data between the BM and the BC501A scintillator. Another NE102A scintillator was mounted in front of the BC501A scintillator as a veto detector to discriminate the charged-particle events.

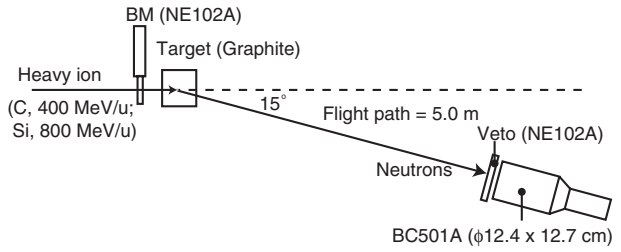

Fig. 1 Schematic of the experimental setup

III. Electronic Circuitry

Data on the pulse height, pulse shape, and flight time were acquired event by event via an electronic circuit connected to a personal computer. **Figure 2** shows the schematic view of the circuit, which consisted of NIM and CAMAC modules. An anode signal from a photomultiplier tube (PMT) combined with the BC501A scintillator was divided into two branches. One of them was fed into a constant-fraction discriminator to generate a logic pulse with a width of 15 ns, and was sent to a coincidence module. If this pulse reached the coincidence module when a logic pulse from the BM with the width of 200 ns was waiting, all the CAMAC modules were activated to acquire the data. Once the data acquisition was started, the processes for new events were inhibited

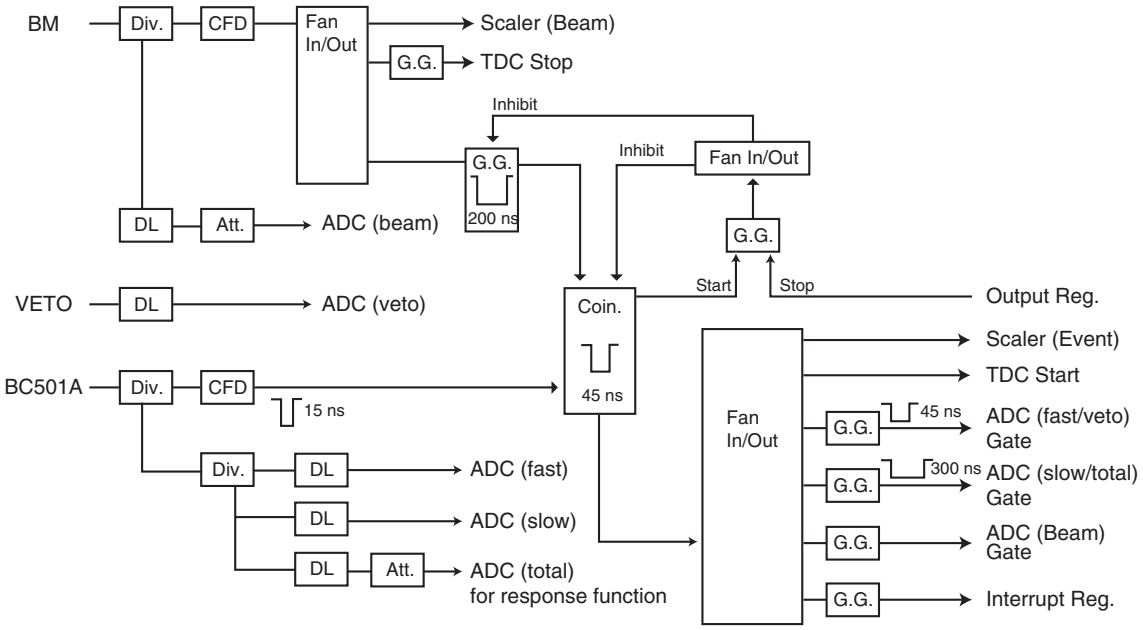

Fig. 2 Schematic of the measurement circuitry
CFD, constant-fraction discriminator; Coin., coincidence module; Output Reg., output register; TDC, time-to-digital converter; G.G., gate and delay generator; Att., attenuator; Div., divider; DL, Delay module.

until the computer gave a release signal through an output register. A time-to-digital converter was used to measure the TOF that corresponded to the time difference between the signals from the BM and the BC501A scintillator. In the present TOF measurements, the delayed signal of the BM was used as a stop signal.

The other branch from the BC501A scintillator was further divided into three, and sent to the charge-sensitive analog-to-digital converters (ADCs). The different gate widths (*i.e.*, 45 ns for a fast gate and 300 ns for the slow and total gates) were set at the ADCs. The slow gate was delayed 150 ns from the initial timing of the fast one. The ADCs with the fast and slow gates were used to eliminate the gamma-ray events with pulse shape discrimination (PSD) by the two-gate integration method. The response function was constructed for the ADC data relative to the total gate signal. In order to obtain the light output spectrum of the veto detector, signals from the veto detector were fed into one of the ADCs whose gate width was set at 45 ns.

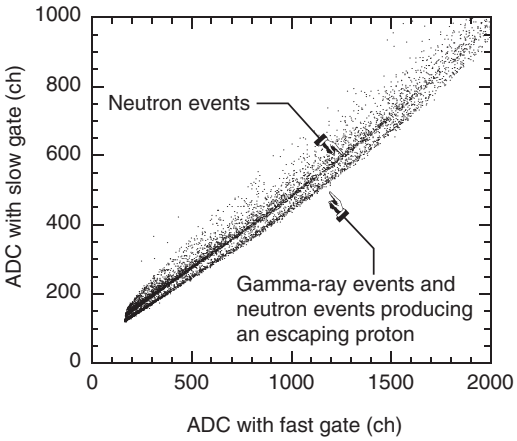

Fig. 4 Result of PSD by the two-gate integration method

IV. Data Analysis

1. Charged-particle Exclusion

The charged-particle events were separated from neutron events using the light output spectrum of the veto detector as shown in **Fig. 3**. The gate of the ADC for the veto detector was opened by a trigger signal from the BC501A scintillator. Even though noncharged particles (*i.e.*, neutrons and gamma rays) passed through the veto detector without interactions, the data for offset of the ADC was taken as the light output of the veto detector. Thereby, a sharp peak by noncharged particles was observed in the low-light-output region corresponding to the offset level of the ADC. On the other hand, charged particles caused luminescence in the veto detector, and they could be successfully distinguished from those of noncharged particles.

2. Neutron and Gamma-ray Discrimination

A typical result of the PSD using fast and slow gates is shown in **Fig. 4**. In an organic scintillator such as BC501A, neutrons and gamma rays are mainly detected as a result of proton recoil and Compton scattering, respectively. Since the energy loss per unit path length (dE/dx) for a proton is larger than that for an electron, the fluorescent tail of a neutron event is longer than that of a gamma-ray event. Hence, the neutron events appear at higher channels than gamma-ray events on the vertical axis in Fig. 4.

Secondary protons produced inside the scintillator by nuclear reactions sometimes escape from the detector wall, and hence deposit only a part of their energies. The pulse shapes for escaping protons are similar to those for electrons because the dE/dx of them are close to electrons. Therefore, the position of neutron events producing an escaping proton are shifted into the region of a gamma-ray event, which makes it difficult to distinguish them. In the present analysis, the events of escaping protons were eliminated from the neutron events together with the gamma-ray events. For consistency, they were also discriminated in the calculations discussed in Chap. V.

3. Energy Determination

The kinetic energies of neutrons were determined by the TOF method. **Figure 5** shows the TOF spectrum for the incidence of 400-MeV/u C ions, where charged-particle events were excluded. Because the stop signal for the TOF measurement came from the BM, in the figure the horizontal

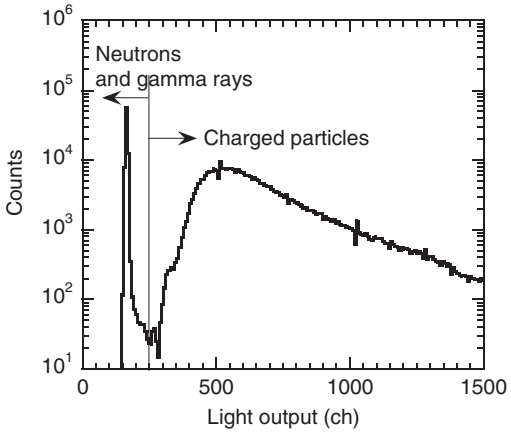

Fig. 3 Light output spectrum of the veto detector

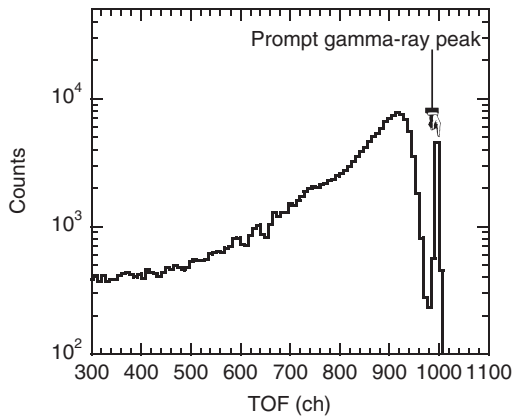

Fig. 5 TOF spectrum for neutrons and gamma rays obtained by the incidence of 400-MeV/u C ions on a graphite target

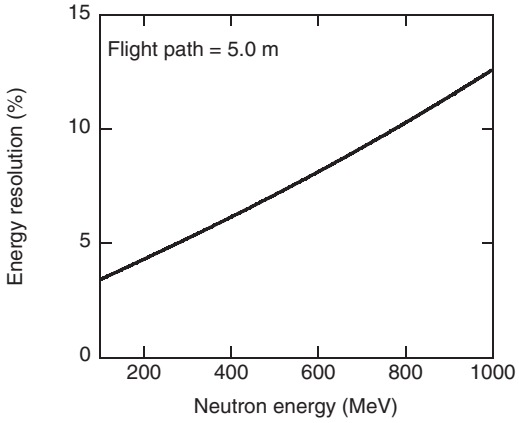

Fig. 6 Energy resolution of TOF measurement

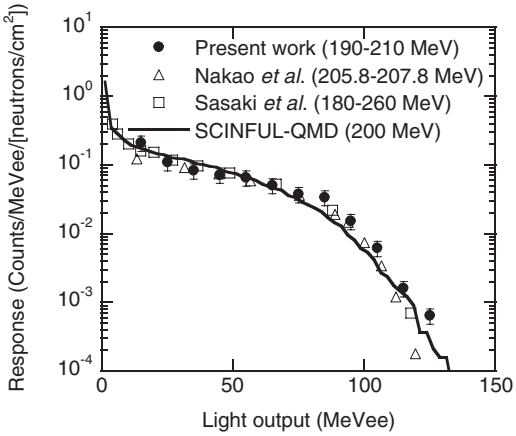

Fig. 7 Measured response function of a BC501A liquid organic scintillator for neutrons of 190–210 MeV

Other experimental data obtained by Nakao *et al.*[12] and Sasaki *et al.*[13] were for neutrons of 205.8–207.8 and 180–260 MeV, respectively. The calculation by SCINFUL-QMD was performed for incident neutrons of 200 MeV.

axis of the TOF spectra is reversed, and hence the prompt gamma-ray peak appears in the right-hand portion of the spectrum. This sharp peak was adopted as a time standard to convert the TOF to the kinetic energy of a neutron.

The uncertainty of the neutron TOF is dominated by the time resolution of the neutron detector. The time resolution of the BC501A scintillator was obtained from FWHM of the prompt gamma-ray peak, and converted into the energy resolution by taking into account the uncertainty of the flight path length. The energy resolution in form of one standard deviation is shown in **Fig. 6**. The typical resolution is 3.4% at a neutron energy of 100 MeV and 10.3% at 800 MeV.

4. Normalization

In order to determine the absolute value of the response function, the number of neutrons entering the BC501A scintillator was estimated from the number of detected neutron events divided by its detection efficiency. In the present analysis, we calculated the detection efficiencies by use of the SCINFUL-QMD code. It should be noted that the detection efficiency is obtained by integrating the response function in the region above a threshold. Though it is difficult to reproduce the complex structure of the response function, the detection efficiency can be estimated with an acceptable uncertainty by the code.

To assess the uncertainty caused by this normalization procedure, the calculated detection efficiencies were compared with the experimental data[12,15] obtained by absolute measurement of the incident neutron fluence. The reported detection efficiencies were 0.047 and 0.051 for neutrons of 206.8 and 388 MeV, respectively, at a threshold setting of 10 MeVee. The corresponding values calculated by SCINFUL-QMD were 0.053 and 0.055. The results of calculation agreed with those of the experiment within 12%. In this work, the uncertainty of the number of incident neutrons was conservatively decided to 15% for energies above 100 MeV.[16,17]

The data from the ADC in units of channels were converted to light output in units of equivalent-electron energy (MeVee). Gamma rays from ^{60}Co and ^{241}Am-Be reference sources were used to determine the calibration points in low-light-output region. In higher light-output region, the calibration was carried out with spallation protons produced inside the target by heavy-ion bombardment. The kinetic energies of the protons were determined from TOF data considering their energy losses during the flight.

V. Results and Discussion

We first examine the validity of our experimental procedure by comparing with other experimental data around 200 MeV, and then show the experimental data in the region of neutrons up to 800 MeV, for which there are no previously available data to test the capability of the code.

The measured response function for neutrons of 190–210 MeV is presented in **Fig. 7** together with experimental data obtained by Nakao *et al.*[12] and Sasaki *et al.*[13] for similar neutron energies. The result of SCINFUL-QMD is also depicted in the figure. The threshold was set at the relatively high level of 20 MeVee because the main purpose of the experiment was to measure neutrons in the high-light-output region. The error bars (equal to one standard deviation) reflect both statistical uncertainties and ambiguities in the number of incident neutrons (15%). The results calculated using SCINFUL-QMD were smeared by a Gaussian function in accordance with the light-output resolution. As mentioned above, the neutron events producing the escaping proton were excluded from the response function in both the experiments and calculations.

The results of the present experiment shown in Fig. 7 agree with other experimental data quite well in both of the shape and absolute magnitude, especially below 100 MeVee within the error bars. This good agreement indicates that our experimental procedure was appropriate. In the comparison between measured and calculated results, SCINFUL-QMD generally reproduces the experimental data well. The agreement is also satisfactory in the low-light-output region, which corresponds to the data of Sasaki *et al.*

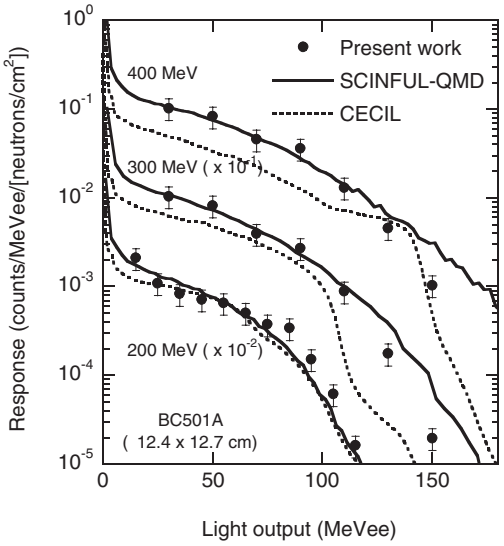

Fig. 8 Response functions for neutrons of 200, 300, and 400 MeV compared with the SCINFUL-QMD and CECIL calculations

The bin width of incident-neutron energies for the experimental data was ±10 MeV (*e.g.*, 290–310 MeV for the result of 300 MeV). Monoenergetic neutrons were used in the calculations.

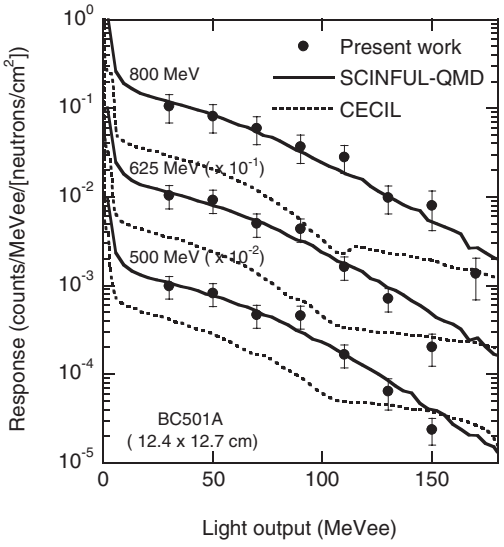

Fig. 9 Response functions for neutrons of 500, 625, and 800 MeV compared with the SCINFUL-QMD and CECIL calculations

The bin width of incident-neutron energies for the experimental data was ±10 MeV (except for 800-MeV neutrons, its width was 750–810 MeV). Monoenergetic neutrons were used in the calculations.

Figures 8 and **9** show response functions for neutrons from 200 to 800 MeV together with the results calculated using SCINFUL-QMD and CECIL.[14] The bin widths for the energies of incident neutrons for the experimental data were ±10 MeV, except for the 800 MeV data (for which a larger bin width was applied in order to accumulate sufficient statistical data). These two figures indicate that the results of SCINFUL-QMD agree with the experimental data very well at all incident-neutron energies, whereas CECIL fails to reproduce the experimental results. This discrepancy is attributable to the simplified treatment of nuclear reactions and particle transport in CECIL. The data of reaction cross sections employed in CECIL are constant above a few hundred million electron volts. Furthermore, protons and alpha particles are the only charged particles considered in the transport and energy deposition processes. The spallation reaction inside the scintillator triggered by the incidence of high-energy neutron is very complex and produces many types of charged particles, including pions. SCINFUL-QMD is able to simulate these reactions more realistically due to its incorporation of a more sophisticated model.[9,10]

These results indicate that SCINFUL-QMD is the most suitable code for calculating the response function at energies above several hundred million electron volts. Indeed, the results calculated using SCINFUL-QMD are acceptable for evaluating the G-function up to 1 GeV. However, the values from SCINFUL-QMD are generally larger than the experimental data at the high-light-output region (above 130 MeVee) in Figs. 8 and 9, with the discrepancy increasing with the incident-neutron energy (becoming twofold at 800 MeV). This problem is attributable to the ambiguity of the light-output database installed in SCINFUL-QMD, which could be solved by updating it.

VI. Conclusion

The response functions of a BC501A liquid organic scintillator have been measured for incident neutrons up to 800 MeV at the Heavy-Ion Medical Accelerator in Chiba (HIMAC) of the National Institute of Radiological Science (NIRS). The experimental data were used to validate the results of the Monte-Carlo-based simulation code SCINFUL-QMD. SCINFUL-QMD generally reproduced the experimental data very well at all incident-neutron energies. A slight overestimation was evident in the high-light-output region, although its contribution to the total response was relatively small. To solve this discrepancy, we will improve the code by obtaining the systematic light-output data for various charged particles.

The present study has experimentally verified the accuracy of SCINFUL-QMD up to 800 MeV. Evaluating the G-function on the basis of SCINFUL-QMD will extend the neutron energies measurable using DARWIN.

Acknowledgments

We express our gratitude to Dr. T. Murakami and the staff operating the HIMAC for their support of our experiments. We also thank Dr. S. Taniguchi, Dr. M. Sasaki, Dr. N. Nakao, and Dr. T. Nakamura for their helpful discussions and advice on this study. This work was performed as a Research Project with Heavy Ions at NIRS-HIMAC, and was partially supported by the Ministry of Education, Science, Sports and Culture by a Grant-in-Aid for Young Scientists (B) (no. 16760692, 2004).

References

1) Joint project team of JAERI and KEK, *The Joint Project for High-intensity Proton Accelerators*, JAERI-Tech 2000-003, Japan Atomic Energy Research Institute, (2000), [in Japanese].
2) Y. Miyamoto, K. Ikeno, S. Akiyama, *et al.*, *Design Concept of Radiation Control System for the High Intensity Proton Accelerator Facility*, JAERI-Tech 2002-086, Japan Atomic Energy Research Institute, (2002), [in Japanese].
3) T. Sato, D. Satoh, A. Endo, *et al.*, "Development of dose monitoring system applicable to various radiations with wide energy ranges," *J. Nucl. Sci. Technol.*, **42**[9], 768 (2005).
4) Y. Oyama, K. Sekiyama, H. Maekawa, "Spectrum weight function method for in-situ fast neutron and gamma-ray response measurements in fusion integral experiments with an NE213 scintillation detector," *Fusion Technol.*, **26**[3], pt2, 1098 (1994).
5) E. Kim, A. Endo, Y. Yamaguchi, *et al.*, "Measurement of neutron dose with an organic liquid scintillator coupled with a spectrum weight function," *Radiat. Prot. Dosim.*, **102**[1], 31 (2002).
6) A. Endo, E. Kim, Y. Yamaguchi, *et al.*, "Development of neutron-monitor detectors applicable to energies from thermal to 100 MeV," *J. Nucl. Sci. Technol.*, **Suppl. 4**, 10 (2004).
7) T. Sato, A. Endo, Y. Yamaguchi, *et al.*, "Development of neutron-monitor detector using liquid organic scintillator coupled with ^{6}Li+ZnS(Ag) sheet," *Radiat. Prot. Dosim.*, **110**, 255 (2004).
8) J. K. Dickens, *SCINFUL: A Monte Carlo based Computer Program to Determine a Scintillator Full Energy Response to Neutron Detection for E_n between 0.1 and 80 MeV*, ORNL Tech. Rep. 6436, Oak Ridge National Laboratory, (1988).
9) D. Satoh, N. Shigyo, Y. Iwamoto, *et al.*, "Study of neutron detection efficiencies for liquid organic scintillator up to 3 GeV," *IEEE Trans. Nucl. Sci.*, **48**, 1165 (2001).
10) D. Satoh, S. Kunieda, Y. Iwamoto, *et al.*, "Development of SCINFUL-QMD code to calculate the neutron detection efficiencies for liquid organic scintillator up to 3 GeV," *J. Nucl. Sci. Technol.*, **Suppl. 2**, 657 (2002).
11) K. Niita, S. Chiba, T. Maruyama, *et al.*, "Analysis of the (N, xN') reactions by quantum molecular dynamics plus statistical decay model," *Phys. Rev. C*, **52**[5], 2620 (1995).
12) N. Nakao, T. Kurosawa, T. Nakamura, *et al.*, "Absolute measurements of the response function of an NE213 organic liquid scintillator for the neutron energy range up to 206 MeV," *Nucl. Instrum. Methods*, **A463**, 275 (2001).
13) M. Sasaki, N. Nakao, T. Nakamura, *et al.*, "Measurement of the response functions of an NE213 organic liquid scintillator up to 800 MeV," *Nucl. Instrum. Methods*, **A480**, 440 (2002); and private communication.
14) R. A. Cecil, B. D. Anderson, R. Madey, "Improved predictions of neutron detection efficiency for hydrocarbon scintillators from 1 MeV to about 300 MeV," *Nucl. Instrum. Methods*, **161**, 439 (1988).
15) Private communication with Dr. S. Taniguchi of Japan Synchrotron Radiation Research Institute (JASRI).
16) K. Ishibashi, H. Takada, T. Nakamoto, *et al.*, "Measurement of neutron-production double-differential cross sections for nuclear spallation reaction induced by 0.8, 1.5 and 3.0 GeV protons," *J. Nucl. Sci. Technol.*, **34**, 529 (1977).
17) D. Satoh, N. Shigyo, K. Ishibashi, *et al.*, "Neutron-production double-differential cross sections of iron and lead by 0.8 and 1.5 GeV protons in the most-forward direction," *J. Nucl. Sci. Technol.*, **40**, 283 (2003).